

## FINITE ELEMENT ANALYSIS OF THE CREEP BEHAVIOUR IN A RESISTANCE SPOT-WELDED JOINT

Ali-Reza Gowhari-Anaraki<sup>\*</sup>, Mohammad K. Pipelzadeh<sup>†</sup> & Stephen J. Hardy<sup>†</sup>

<sup>\*</sup>Department of Mechanical Engineering,  
Iran University of Science & Technology,  
Tehran, Iran  
E-mail: [gohari@mech.iust.ac.ir](mailto:gohari@mech.iust.ac.ir)

<sup>†</sup>School of Engineering,  
University of Wales-Swansea,  
Singleton Park, Swansea SA2 8PP,  
United Kingdom. TEL: +44-1792-295570 FAX: +44-1792-295676  
E-mail: [m.k.pipelzadeh@swan.ac.uk](mailto:m.k.pipelzadeh@swan.ac.uk)  
E-mail: [s.j.hardy@swan.ac.uk](mailto:s.j.hardy@swan.ac.uk)

**Key words:** Spot-Welded Joint, Finite Element Analysis, Solid Elements, Creep Analysis

**Abstract.** *This paper describes the elastic-plastic-creep analysis of a resistance spot-welded joint using the finite element method. A solid element model representing the spot-weld has been considered and is subjected to shear-tension, peel and cross-tension loading. The creep analysis is studied on a typical geometry that is widely used in experimental laboratories. The creep behaviour around three points in the spot region and one point remote from the critical region is studied. A constant temperature of 690 degrees and time duration of up to 100 hours have been considered. The creep material model is based on the Norton-Bailey law. The creep stress-strain predictions are compared with simplified notch creep stress-strain conversion (NCSSC) rule estimates. It was found that the Neuber rule provides conservative estimates.*

## 1 INTRODUCTION

Geometric discontinuities in engineering components such as holes, grooves, flanges, welded joints (the subject of this investigation) induce local high stresses. These are generally known as 'notches' and are likely sites for plastic formation under moderate to high loading. They are the main source of crack initiations followed by subsequent propagation and sudden failure. Design assessments must take account of any such stress raisers where many instances of mechanical failures can be attributed to inadequate design in the region of a discontinuity. Spot-welded lap joints are used extensively in the fabrication of thin sheet-metal vehicle structures, such as automotive bodies and railway rolling stock. The strength of these structures is very dependent on the spot-welds which are likely to be subjected to mechanical and/or thermal loading.

The study of the creep behaviour of notched components subjected to high temperatures has been performed by many researchers. In 1980, Dawson et al<sup>1</sup> compared experimental results with the elastic-plastic finite element predictions of the creep behaviour of axially loaded shouldered tubes. They tested four lead-based-alloy models and used strain gauges to measure the creep strain on the shoulder at a temperature of 610°. Their comparison was in good agreement with the finite element. Webster and Pickard<sup>2</sup> obtained methods for the creep rupture life of notched components. They considered a circumferential V-shaped component and a plate with semi-circular notches at the top and bottom sides. They used three methods for analysis, these including the elastic, elastic-plastic and elasto-plastic-creep. The variations of axial and equivalent stresses for each method away from the root of the notch were presented. Also, variations of the creep strain with respect to time at the critical points in the notch and away from it were plotted. Both the finite element and experimental results were in close agreement. Sluzalec and Kysiak<sup>3</sup> studied the analysis of the weld geometry in creep of welded tubes undergoing internal pressure. Their paper contained non-linear thermodynamic formulations, creep related laws and the flow rules. The authors looked into four important aspects of the spot-weld, such as the spot-weld material, area under thermal effect and the root of the weld. The analysis of the stresses in these regions was investigated using thermo-elastic-plastic finite element analysis. They presented the radial, axial and hoop stress distributions along the line of symmetry of the weld at various time intervals. Colombo et al<sup>4</sup> analyzed the creep and damage in the intersection plane of T-shaped branch pipes of a boiler-head. They compared finite element analysis with experimental tests. The finite element analysis was based on the continuous damage mechanics and data taken from experiments on the creep and creep-rupture life, in order to describe the prediction of crack initiation in the stressed region. Segle et al<sup>5</sup> presented results on the estimation of the longitudinal seam welding life, based on experimental creep tests using cross-weld specimens. The choice of correct pipe diameter in predicting the behaviour of longitudinal-weld necessitated the use of experimental tests on the cross-welded components. They found that the damage-mechanics method is more accurate than other considered methods in determining the life and position of the creep rupture.

In the present study, the finite element method is used to analyze the creep behaviour of a single spot lap joint subjected to shear-tension, peel-tension and cross-tension loading and at a

temperature of 690°. These forms of loadings are the most likely to cause failure. A typical geometry with relatively moderate stress concentration factor (SCF) is considered to study the elastic-plastic behaviour of the spot-weld joint using a solid element model. This model is found to be more accurate than other forms of representations of the spot-weld nugget<sup>6,7</sup>. For post yielding, the local regions of high stress are relieved as yielding occurs and results in the formation of a plastic zone. Therefore a criterion based on the accumulation of strain must be used in order to assess the creep behaviour of the spot-weld. Finite element analysis is expensive and time consuming. Alternatively, simple numerical relationships have been proposed. These are known as notch creep stress-strain conversion (NCSSC) rule estimates. Typically Neuber<sup>8</sup>, Linear and the intermediate rules<sup>9</sup> are used to estimate the strain values.

### 1.1 Notation

A, B	Creep constants
d	Spot-weld mean diameter
U	Displacement
E	Elastic modulus
I	Index
$K_t$	Elastic stress concentration factor
$K_\epsilon$	Elastic-plastic strain concentration factor
$K_\sigma$	Plastic stress concentration factor
L	Plate length
m,n	Creep constants (function of temperatures)
t	Plate thickness
$t_r$	Creep rupture time
T	Time
W	Plate width (Distance between two consecutive weld-spots)
$\epsilon^c$	Creep strain
$\dot{\epsilon}_{min}^c$	Rate of creep strain
$\sigma$	Stress
$\nu$	Poisson's

### Subscripts

n	Nominal
max	Maximum
o	Initial
sgn	Sign of
X, Y,Z	Coordinate directions

## 2 LOADING AND BOUNDARY CONDITIONS

Figure 1 shows a typical mesh of a half of the model with loading and boundary conditions.

The basic shape of the component is made from two lapped plates with a single centrally-positioned spot-weld joining the two plates. The geometry of the spot-welded joint is described by four dimensions; the plate length,  $L$ , the plate width,  $W$ , the plate thickness,  $t$  and the spot-weld mean diameter,  $d$ . A typical geometric component with the following dimensions was considered:

$D= 5$  mm,  $W=25$  mm,  $L= 25$  mm and  $t=1$  mm.

Three types of loading are considered. These are as follows:

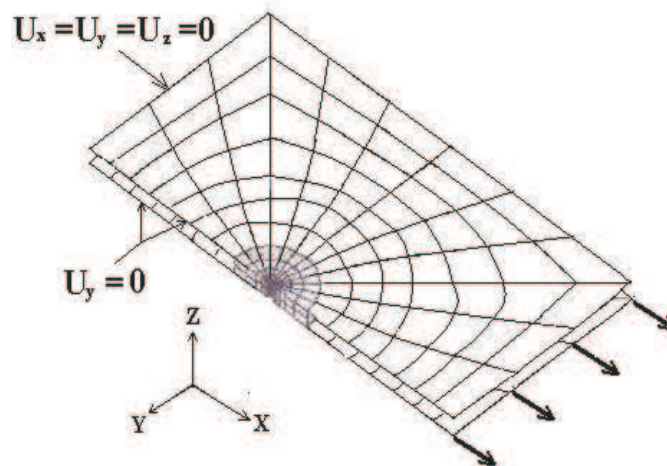
- 1- Shear-tension loading,
- 2- Peel-tension loading,
- 3- Cross-tension loading.

These loads are commonly applied in many applications in the automotive industry and are the most prevalent in the failure of spot-welded joints.

For all load cases considered, the line of symmetry of the joint is prevented from displacing in the plane normal to the applied loads (i.e.,  $U_y=0$ ). Additional boundary conditions are imposed depending on the type of load. These are clearly shown in Figure 1. Both loads and boundary conditions are applied to the free ends of the plates.

### 3 FINITE ELEMENT ANALYSIS

In all cases considered, the plates were represented using four-noded quadrilateral thin plate elements with the integral Gauss points 2 by 2 array. However, the weld nugget region has been modelled using eight-noded and six-sided solid elements with the integral Gauss points of 2 by 2 by 2. A typical finite element mesh is shown in Figure 1. Due to the symmetry of the



(a) Shear-tension

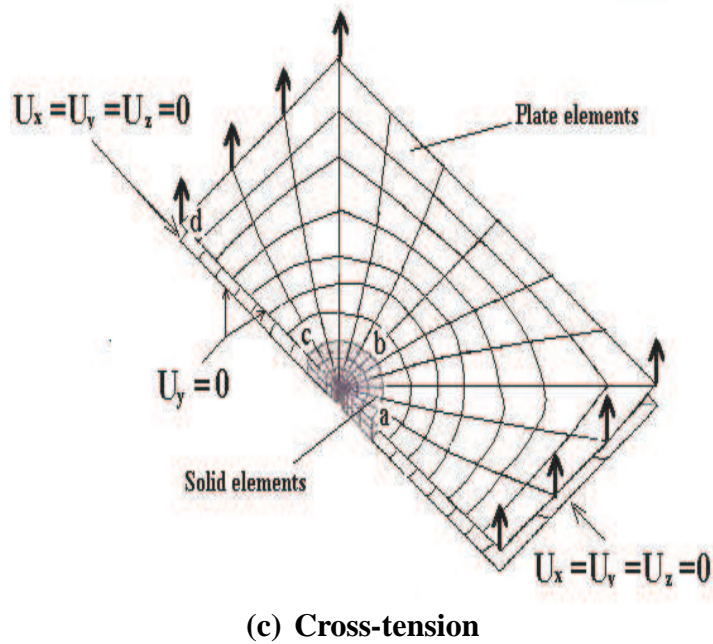
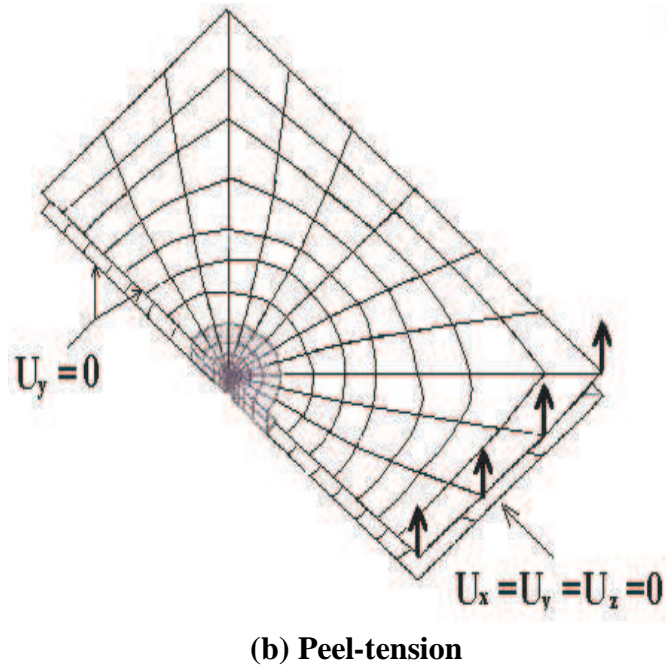


Figure 1: Finite element models of half of the spot-welded joint with the applied constraints and (a) shear-tension, (b) peel-tension and (c) cross-tension loading.

component, a half model of the joint has been considered. Predictions from this model<sup>6,7</sup> were

found to be in close agreement with the experimental results. All analyses were carried out using the standard elastic-plastic facilities of the NISA II software package<sup>10</sup>. A refined mesh is employed in the critical region of the spot-weld with an average of 420 elements and 640 nodes.

The size of the elements was based on the following factors:

1- From the elastic analysis, the maximum stress at the root of the notch is identified from which the elastic stress concentration factor,  $K_t$ , is determined. The number of elements is increased and its effect on  $K_t$  is monitored. The final mesh size is chosen when  $K_t$  becomes constant,

2- The stress discontinuities at the inter-elements boundaries along the line of symmetry are considered and compared. The refined mesh gave a stress discontinuity at the common nodal points of less than 5 percent and therefore considered to be appropriate for the analysis.

For the creep analysis, the material behaviour is based on the iterative method of the Norton-Bailey law<sup>11</sup>, which is expressed as:

$$\varepsilon^c = A \left( \frac{|\sigma|}{\sigma_o} \right)^m \left( \frac{T}{T_o} \right)^n \text{sgn } \sigma \quad (1)$$

where;  $A = 1.883E-6$ ,  $\sigma_o = 70$  MPa,  $m = 2.54$  and  $n = 0.452$ .

On average, three iterations were required for convergence. For the considered loadings, 41 time increments were used. Throughout the analysis, mechanical properties of Young's modulus and Poisson's ratio of  $E = 190$  GPa and  $\nu = 0.33$  respectively were assumed.

## 4 RESULTS

In the analysis of the creep behaviour of the spot-weld, the following results are presented:

- 1- Strain distributions along the line of symmetry and around the weld nugget at 4 points, three of which are located in the periphery of the weld nugget (points a, b, c and d in Figure 1(c)) and the fourth point which is placed remotely from the weld for the range of time,
- 2- Variations of strain at the critical and non-critical points around the spot-weld with respect to time,
- 3- Variations of stress at the critical and non-critical points around the spot-weld with respect to time.

Figure 2(a) shows the creep strain distributions in the longitudinal direction up to 100 hours for shear-tension loading. The distributions are taken at 0.1, 1, 10 and 100 hours. Similarly, Figures 2(b) and 2(c) show the creep strain distributions for peel and cross-tension loading respectively. For all loadings considered, the variations initiate near the edge of the weld-nugget and reach the maximum at the other end of the weld-nugget close to the applied load. Beyond the peak points, the variations in creep stain reduce drastically.

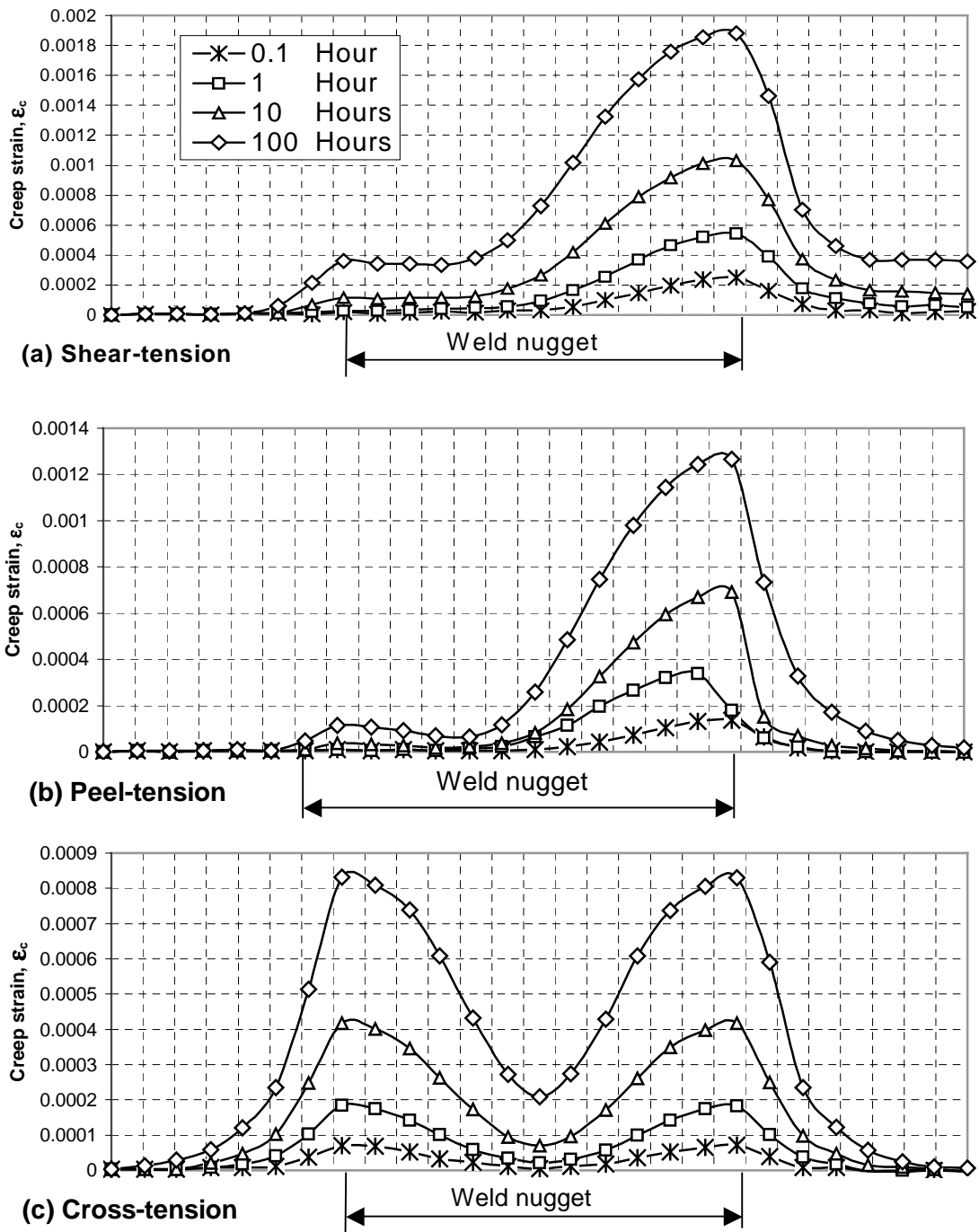
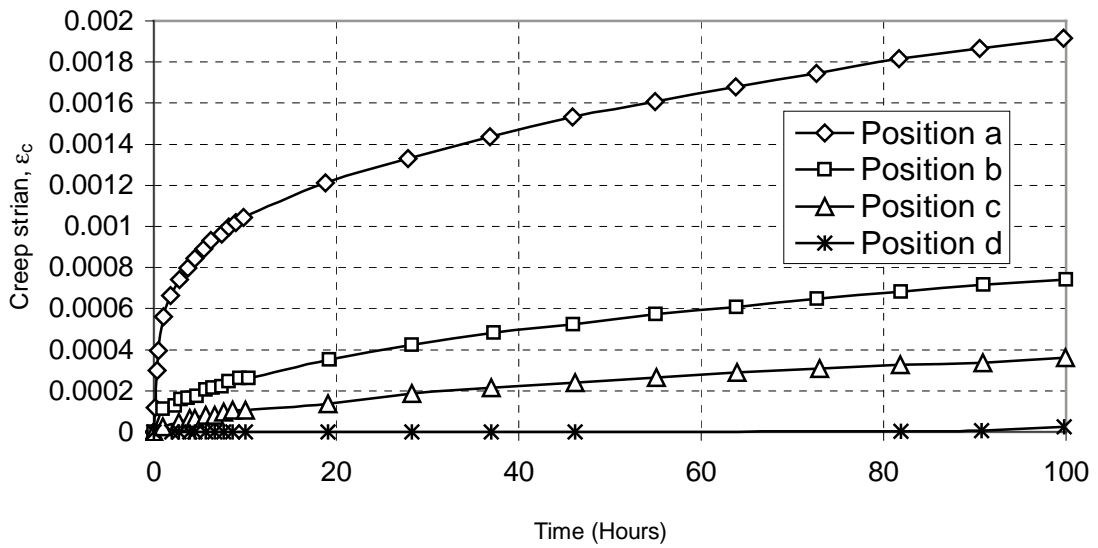


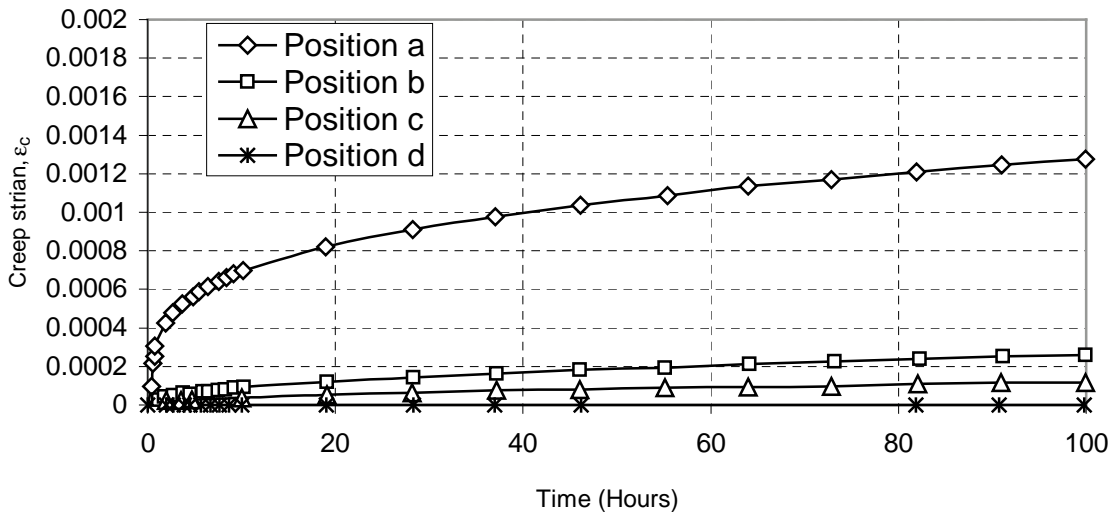
Figure 2: Distributions of creep strain around the spot-weld under (a) shear-tension, (b) peel-tension and (c) cross-tension loading at various time durations.

Figure 3 shows creep strain variations at the four considered points. For all load cases, the

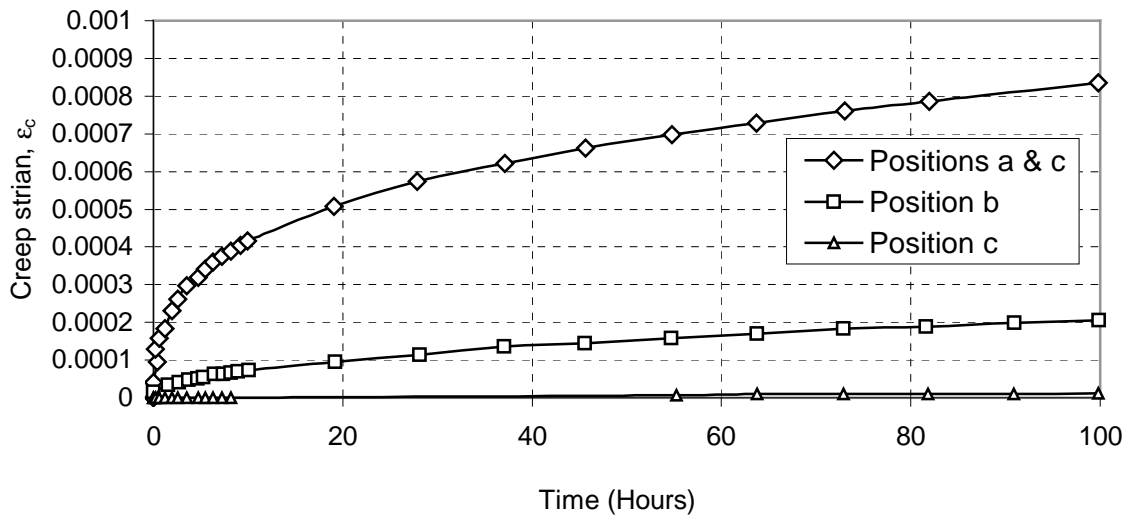
creep strain increases rapidly for the first 10 hours. After 10 hours, point ‘a’ gives a steady increase in the strain with respect to time (see Figure 1(c)), whereas, others points exhibit a constant value of strain with the time. The creep strain in point ‘d’, away from the weld-nugget, was negligibly small. For both shear-tension and peel-tension loads, the maximum creep strain occurred at point ‘a’ of the weld nugget. Whereas, for the cross-tension load, the peak stain occurred at points ‘a’ and ‘c’. This is due to the symmetric nature of the load and geometry. Also, Figure 3 clearly shows that the longer the duration the weld is subjected to the temperature, the higher the magnitude of the creep strain.



(a) Shear-tension



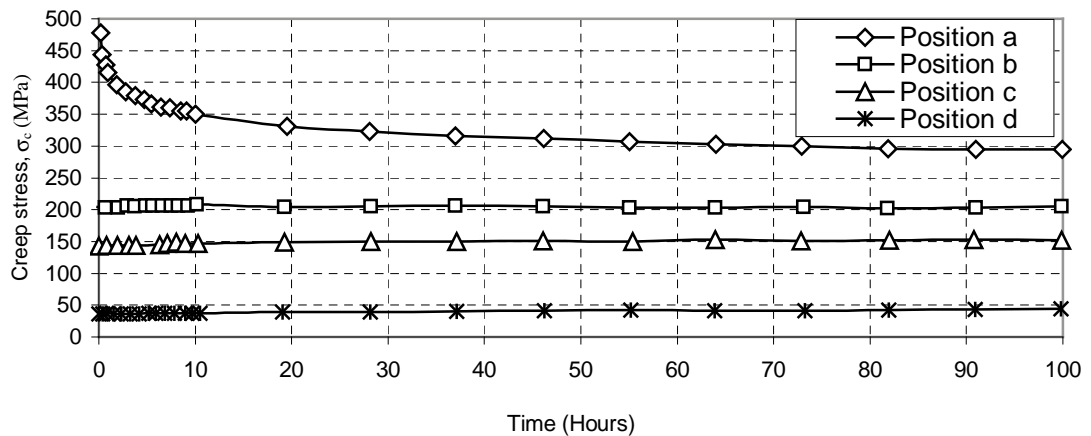
(b) Peel-tension



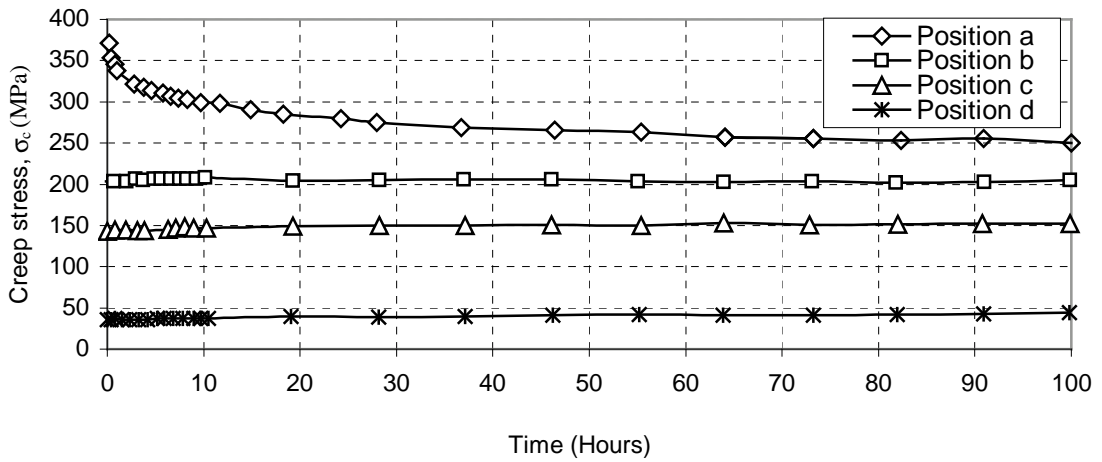
(c) Cross-tension

Figure 3: Variation of creep strain with time for (a) shear-tension, (b) peel-tension and (c) cross-tension loading at various points.

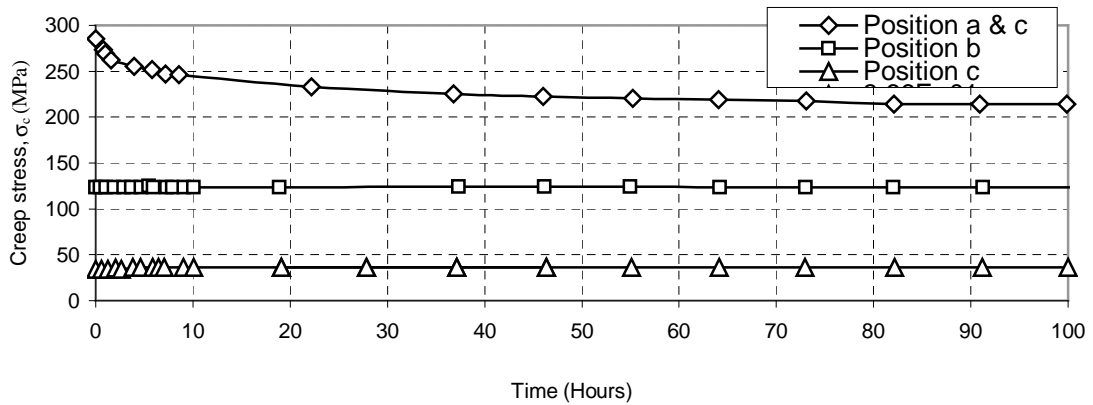
Figure 4 shows the variations of the creep stress with respect to time at the four considered points. For all load cases considered, the general trends are opposite to the corresponding creep strain. This is clearly noticeable for point 'a'. However, other points show constant creep stress and therefore are independent of time. For both the creep stress and strain, the maximum occurred in point 'a'. These results are considered in the next section on determining the index 'I'.



(a) Shear-tension



(b) Peel-tension



(c) Cross-tension

Figure 4: Variation of creep stress with time for (a) shear-tension, (b) peel-tension and (c) cross-tension loading at various points.

#### 4.1 Comparison of finite element predictions with the numerical relations

The life of components under creep conditions, expressed as the rupture time,  $t_r$ , is an important design parameter. Generally, increasing the temperature and the nominal load will result in the reduction of the rupture time,  $t_r$ . Many researchers attempted to present a relationship between rate of creep stain,  $\dot{\epsilon}_{min}^c$ , creep stress and temperature, also, a relationship between  $t_r$ , creep stress and temperature. The most important relation is the work of Monkman and Grant<sup>12</sup>. They have obtained the following logarithmic expression after conducting many experiments on metals:

$$\text{Log } t_r + m \text{Log } \dot{\epsilon}_{min}^c = B \quad (2)$$

where  $t_r$  is the creep rupture time (i.e. failure time),  $\dot{\epsilon}_{min}^c$  is the rate of the steady-state creep

strain,  $B$  and  $m$  are constant coefficients. For certain metals with bases of steel, aluminium, copper and nickel, coefficients  $B$  and  $m$  are found to be in the following range:

$$\begin{aligned} 0.48 < B < 1.30 \\ 0.77 < m < 0.93 \end{aligned} \quad (3)$$

From Equation 2, the failure life can be easily estimated, provided  $\dot{\varepsilon}_{\min}^c$  is known. Unfortunately, the estimation of  $\dot{\varepsilon}_{\min}^c$  requires solving a non-linear creep behaviour. Hence, for complicated components, it will be expensive and time consuming.

The main objective of this paper is the presentation of a simple method to estimate  $\dot{\varepsilon}_{\min}^c$  and the creep stress without performing a complicated non-linear analysis or prototype experimental test. Such a relationship is known as Notch Creep Stress-Strain Conversion rule (NCSSC) which is expressed by<sup>13</sup>:

$$\frac{K_{\varepsilon}}{K_t} = \left( \frac{K_t}{K_{\sigma}} \right)^I \quad 0 < I < 1 \quad (4)$$

When index 'I' is set equal to zero or one, it will represent the Linear or Neuber rule respectively. However, the Intermediate rule applies when index 'I' lies between these two extreme values. Parameter  $K_t$  is the geometric elastic stress concentration factor obtained under mechanical loading only.  $K_{\sigma}$  is the plastic stress concentration factor which is obtained by dividing the peak stress (i.e. point 'a' of Figure 4) at the root of the spot-weld at a considered time by the nominal stress, again, under mechanical loading conditions.  $K_{\varepsilon}$  is the elastic-plastic strain concentration factor and is the ratio of the maximum total creep strain (i.e. point 'a' of Figure 3) at the root of the spot-weld at a considered time to the nominal strain, again, obtained under mechanical loading.

$$i.e. \quad K_{\sigma} = \frac{\sigma_{\max}}{\sigma_n} \quad \& \quad K_{\varepsilon} = \frac{\varepsilon_{\max}}{\varepsilon_n} \quad (5)$$

Hence, index 'I' is calculated as:

$$I = \text{Log} \left( \frac{K_{\varepsilon}}{K_t} \right) / \text{Log} \left( \frac{K_t}{K_{\sigma}} \right) \quad (6)$$

$K_t$  values are equal to 6.15, 3.15 and 2.8 for the shear-tension, peel-tension<sup>7</sup> and cross-tension loading respectively. All  $K_t$  values are obtained under mechanical loading.

Using these rules (i.e. in the form of Equation 4) and knowing the material creep stress-creep strain behaviour at a particular temperature, the creep stress and creep strain at the critical point in the spot-weld can be estimated. Then, from, the creep stress-rupture time

curves, the creep life is obtained.

Figure 5 shows the derived 'I' values based on the finite element prediction of stress and strain with time for the three loading cases considered. The general trends of the index 'I' with respect to time are similar to the maximum creep stress at the critical point (i.e. point 'a'). The range of 'I' values were found to be between 0.62 and 1.38 with an overall average value of 0.87.

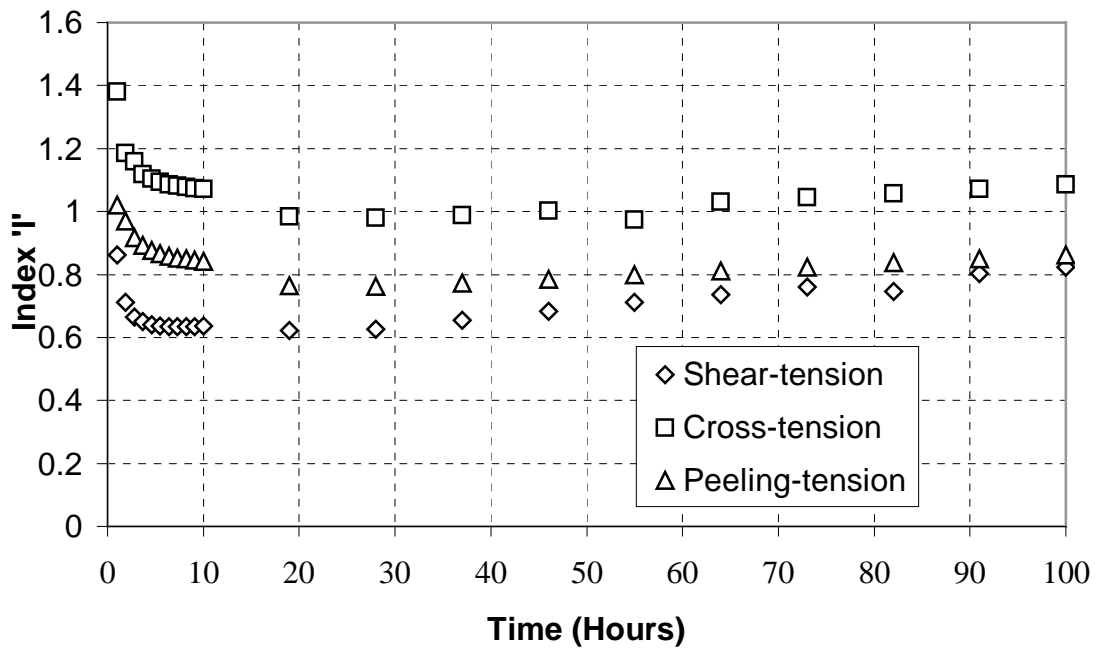


Figure 5: Variation of the index 'I' with time for various loads.

## 5 SUMMARY OF CONCLUSIONS

1- The results have shown that for the spot-welded joint considered with the low stress concentration factor under creep condition, the Neuber rule appears to give a reasonable estimate of the creep strain. This is consistent with the elastic-plastic analysis of plates under axial loading with low  $K_t$  values<sup>14</sup>,

2- The finite element analysis of the spot-welded joint using the solid element model under high localised stresses has shown that an intermediate rule with the index 'I' set equal to 0.87 will give a better estimates of the creep strain.

3- For all loadings considered, increasing the temperature will results in an increase in the creep strain accompanied by a reduction in creep stress. The shear-tension and cross-tension loads gave the upper and low creep stress & strain values respectively. Under creep conditions, all the stress and strains with respect to time for various loading conditions were found to follow similar trends

## 6 REFERENCES

- [1] Dawson, R.J., Fessler, H., Hyde, T. H. and Webster J. J., "Elasto-plastic and creep behaviour of axially loaded, shouldered tubes", *J. Strain Analysis*, **15** (1), 21-29, (1980).
- [2] Webster, P. S. and Pickard, A.C. "The prediction of stress rupture life of notched specimens in the beta - processed titanium alloy TU53 Is", *J. Strain Analysis*, **22** ( 3), 145-153, (1987).
- [3] Sluzalec, A. and Kysiak, A. "An analysis of weld geometry in creep of welded tubes undergoing internal pressure". *J. Computer & Structures*, **40**, (4), 931-938, (1991).
- [4] Colombo, P.P., Garzillo, A., Meriggi M., Ponzoni, C. and Sampietri, C., "Creep and damage analysis of a serviced the intersection in a boiler header: comparison between numerical and experimental results", *Int. J. Press. Ves. & Piping*, **66** (1), 243-251, (1995).
- [5] Segle, P., Tu, T. T, Storesund, J. and Samuelson, L. A. , "Some issue in life assessment of longitudinal seam weld based on creep test, with cross - weld specimens", *Int. J. Pres. Ves. & Piping*, **66** (1), 199-222, (1996).
- [6] Pal, K. and Cronion, D. L., "Static and dynamic characteristics of spot-welded sheet metal beams", *Vibration of mechanical systems and history of mechanical design*, **63**, AMSE, 97-104, (1993).
- [7] Gowhari-Anaraki, A. R., Pipelzadeh, M. K. & Hardy, S. J., "Experimental and numerical analysis of low cycle fatigue of Spot-welded joints under peel-tension loading", *MECOM 2002*, First South-American Congress on Computational Mechanics, Santa Fe-Parana, Argentina, pp. 784-804, (2002).
- [8] H. Neuber, "Theory of stress concentration for shear strained prismatical bodies with arbitrary nonlinear stress-strain law", *J. Applied Mech.*, **28**, 544-550, (1961).
- [9] H. O. Fuchs and R. I. Stephens, *Metal Fatigue in Engineering*, J. Wiley and Sons, N. Y., (1980).
- [10] NISAI, *user manual*, Engineering Mechanics Research Corporation, (1992).
- [11] Penny, R.K. and Marriott, D.L., *Design for creep*, McGraw-Hill book company (LTK) Limited, London, (1971).
- [12] Monkman, F.C. and Grant, N.J., *Proc. ASTM*, **56**, 593 (1956).
- [13] Gowhari-Anaraki, A.R. and Hardy, S.J., "Low cycle fatigue life predictions of hollow tubes with axially loaded axisymmetric internal projections". *J. Strain Analysis*, **26**, 133-146, (1991).
- [14] Hardy, S. J. and Pipelzadeh, M. K., "Elastic-plastic finite element analysis of short flat bars with projections subjected to axial loading", *Journal of Strain Analysis*, **31**, 25-32, (1996).